Chapter 6

On the Co-ordination of Granular Rods

6.1 Introduction

In any random packing, the number of touching neighbors per particle, or the co-ordination number is an important quantity because contacts between particles provide the necessary mechanical constraints to ensure a stable pile. In this chapter the average co-ordination number for random packings of rods is measured as a function of the rod aspect ratio. A statistical theory of granular rods is needed in order to relate the co-ordination number to the collective behavior of the packing. The random contact model discussed in Section 1.1.3 provides this theoretical framework. The co-ordination number measurements along with measurements of the collective behavior of granular rod packings are used to evaluate the validity of the random contact model.

The average co-ordination number for a given pile is:

$$\langle z \rangle = \frac{\sum_z n_z z}{\sum_z n_z} \tag{6.1}$$

where n_z is the number of rods with z neighbors. The fraction of rods which have a given co-ordination number is $\gamma_z = n_z / \sum_z n_z$ so that the normalization condition $\sum_z \gamma_z = 1$ is met. γ_z as a function of z is the co-ordination number distribution function.

In an isostatic pile the number of constraints, or contacts per particle, equals the number of force and torque balance equations [83]. For an isostatic packing of frictionless spheres in d dimensions the number of contacts equals the number of force balance equations $\langle z \rangle = 2d$. For frictional spheres each contact determines two equations so that $\langle z \rangle = d + 1$ [84]. This result holds for frictional particles of any shape so that in 3 dimensions, the isostatic frictional limit yields $\langle z_f^{\text{iso}} \rangle = 4$ [85] although there is some debate about whether or not this argument is strictly valid for non-spherical particles [78] . For frictionless rods in 3 dimensions: $\langle z_n^{\text{rod-iso}} \rangle / 2 = 3 + 2$ so that $\langle z_n^{\text{rod-iso}} \rangle = 10$.

Bernal & Mason [86] measured $\langle z^{\text{sph}} \rangle = 6.4$ for a random packing of spheres. Their result for $\langle z^{\text{sph}}$ is close to the isostatic limit for frictionless spheres. Their method was to pour spheres into a container, pour paint into the container, drain the paint, allow the pile to dry and then count the number of spots on each sphere without any paint. Such spots represent touching neighbors. This is a tedious process. More than forty years later Donev *et al.* [78] made the subsequent experimental measurement of $\langle z^{\text{M\&M's}} \rangle = 9.8$ using Bernal & Mason's method on oblate ellipsoids with an aspect ratio of 2 (M&M's Candies [87]), which is near the isostatic limit for frictionless spheroids. Note that neither Bernal & Mason [86] nor Donev *et al.* [78] controlled for or varied friction experimentally. If piles of granular cylinders behave similarly to spheres and ellipsoids in approaching the isostatic limit then one expects $\langle z \rangle \sim 10$ independent of rod aspect ratio.

Donev *et al.* [78] also performed frictionless simulations of random packings of ellipsoids and showed that $\langle z \rangle$ has a minimum for spheres and increases sharply as

spheres are deformed into ellipsoids. Their simulations demonstrate that $\langle z \rangle \sim 10$ for maximally jammed random [88] packings of frictionless prolate and oblate ellipsoids at an aspect ratio of approximately two where the aspect ratio of an ellipsoid is defined as the ratio of its major to minor axes. Their simulation results show that although the symmetry of particles changes abruptly as the aspect ratio is changed from unity (spheres), the average contact number changes smoothly as a function of aspect ratio. The curvature of the contact number as a function of aspect ratio is not well understood.

Simulations of granular rods in two dimensions [77] show that $\langle z \rangle$ decreases as the rod aspect ratio increases towards an asymptotic value of $\langle z^{2d} \rangle = 3.2$. Philipse & Verberkmoes presented a frictionless and purely geometric argument for random packings of rods in three dimensions and calculated a lower bound of $\langle z \rangle = 5$ [89]. Williams & Philipse [90] performed frictionless monte carlo simulations of random rod packings in three dimensions and found that $\langle z \rangle$ decreased towards the frictional isostatic limit with increasing rod aspect ratio, which is opposite to our experimental measurements.

As mentioned in Section 1.1.3, Philipse [15] presented experimental data on compacted piles of granular rods showing that the product of the pile's volume fraction (ϕ) and the ratio of the rod's length (L) to the rod's diameter (D) is a constant $\phi \times (L/D) = c$, for long, thin rods ($L/D > 20$) meaning that low volume fractions can be achieved experimentally ($\phi \approx 0.06$ for $L/D = 96$). As discussed in Section 1.1.3 Philipse [15] showed that the random contact model, described in Section 1.1.3, predicts this scaling. In this chapter the RCM is experimentally tested by measuring $\langle z \rangle$, L/D and ϕ.

6.2 Materials & Methods

Compaction experiments were performed to measure ϕ as a function of L/D by pouring rods into a container and then compacting the pile by vertical excitation of the container with a single period of a 50 Hz sine wave at a maximum acceleration of five times gravity. The excitation was repeated at a rate of 1 Hz for 10^3 excitations. Cut pieces of tinned buss wire with diameters ranging from 0.25 mm to 1.4 mm were used for compaction experiments and for the co-ordination number experiment with $L/D = 3$. A Schleuniger RC 3250 cable cutter cut spools of round wire to make the rods. These wire pieces have $\Delta L/L = 1\%$ polydispersity in length. Each experiment was repeated three times and the volume fraction was taken to be the average of the three trials. A quasi-steady state was reached after typically 500-1000 excitations but further compaction was not systematically investigated. The evolution of the piles' volume fraction as a function of number of excitations is shown in Fig. 6.1. Note that the rods in these piles never aligned vertically in a layered packing as did the $L/D = 3$ rods in the experiments of Villaruel *et al* [76] who showed that typically 10^4 excitations were needed to align short rods after compaction of randomly oriented piles. Long rods form highly jammed piles in which local particle rearrangements are constrained. Rods in the bulk of such piles do not rearrange when the pile is vertically vibrated. Of course, even large aspect ratio rods will flow align when poured into very small containers as do pieces of spaghetti in a thin box [79]. The volume fraction of the compacted piles scales as $\phi_{\text{comp}}(L/D) = 5.4 \pm 0.3$ as shown in Fig. 6.3, which is consistent with previous results [15], and for uncompacted piles as $\phi_{\text{uncomp}}(L/D) = 4.2 \pm 0.2$ as shown in Fig. 6.2.

In order to measure $\langle z \rangle$ for random rod packings we followed Bernal & Mason's method. Wooden toothpicks and bamboo skewers with circular cross-sections were used as the granular rods in piles for which $\langle z \rangle$ was measured. The toothpicks measure 0.2 cm in diameter and 6.5 cm in length with pointed ends. The bamboo

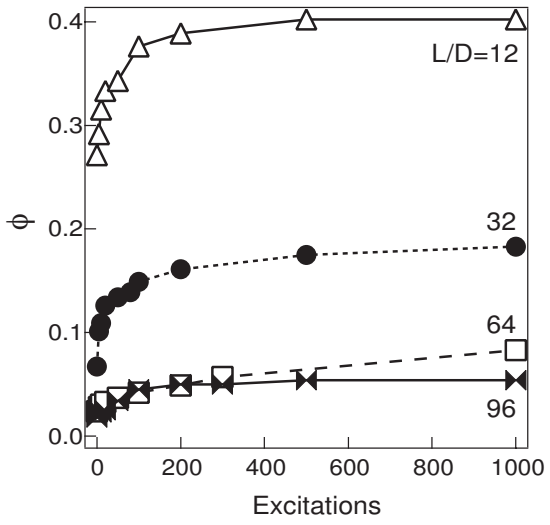

Figure 6.1: The volume fraction ϕ of piles of granular rods is shown as a function of the number of vertical excitations for L/D =12, 32, 64 and 96.

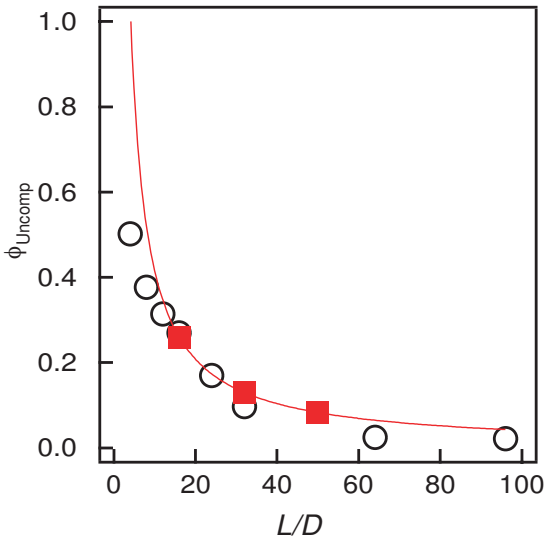

Figure 6.2: The dependence of the initally poured, uncompacted volume fraction ($\phi_{\rm Uncomp}$) as a function of L/D is shown. The data from bulk compaction experiments are shown as open circles and the data from co-ordination number experiments are shown as filled squares. The solid line is $\phi \times (L/D) = 4.2$.

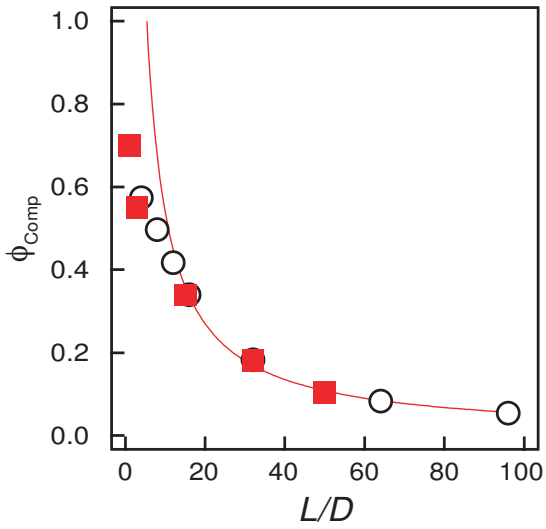

Figure 6.3: The dependence of the final, compacted volume fraction (ϕ_{Comp}) as a function of L/D is shown. The data from bulk compaction experiments are shown as open circles and the data from co-ordination number experiments are shown as filled squares. The solid line is $\phi \times (L/D) = 5.4$.

skewers measured 0.26 cm in diameter and were cut to 4 and 13 cm lengths to provide L/D=15 and 50 rods. The measured polydispersity in the toothpicks' length was approximately 2% and 3% for the bamboo skewers. We used Jujube candies [91] as L/D=1 rods. Jujubes approximate the shape of right cylinders of L/D=1. The polydispersity of Jujubes is $\Delta L/L = 20\%$ and $\Delta D/D = 10\%$. This large polydispersity leads to more contacts on average than for a monodisperse pile. Aluminum disks of 1.27 cm diameter were used as rods of aspect ratio $L/D = 0.4$. It must be noted that the compacted pile of disks displayed local parallel orientational ordering although the entire pile was isotropic [92]. 17% of disks aligned parallel to their neighbors in chains of 2-5 particles forming extended contacts across the circular faces of the disks. An extended contact between disk faces was counted as three contacts in the co-ordination number distribution. The fraction of chains of 2, 3, 4, and 5 particles was 0.74, 0.21, 0.03 and 0.02 respectively, showing that the vast majority of chains were made up of two or three particles. No extended cylindrical edge to face contacts

were observed. These aluminum disks had polydispersity of 2% both in length and diameter.

Those rods which contacted the container walls or exposed upper surface of the pile were categorized as boundary particles and those which did not were categorized as bulk particles. The compacted pile of toothpicks used to measure $\langle z \rangle$ after removal from the container is shown in Fig. 6.4. The boundary particles are clearly aligned whereas the bulk particles appear to be randomly oriented. The measured co-ordination number distribution for this pile of toothpicks is shown in Fig. 6.5. The co-ordination number distributions are qualitatively similar for all rod aspect ratios and pile volume fractions. The center of the distribution shifts as a function of aspect ratio but the width of the distribution remains constant within experimental error. As shown in Fig. 6.5, the co-ordination number distribution for boundary particles is shifted to a lower value of $\langle z \rangle$ relative to that for bulk particles and is slightly asymmetric due to the lower limit on z. Rods which contact the boundary must have fewer contacts with other rods than rods which do not contact the boundary which explains the shift to a lower $\langle z \rangle$ value. The asymmetry in the co-ordination number distribution for boundary rods is due to the presence of a lower cutoff: no rods were observed to have $z < 2$, whereas no upper cutoff independent of L/D was observed. Table 6.1 lists the measured values of $\langle z \rangle$ for compacted and uncompacted piles of different aspect ratio rods as indicated including only the bulk rods.

6.3 Results

The average co-ordination number for random right cylinder packings increases as a function of aspect ratio from $\langle z \rangle \sim 6$ for disks of aspect ratio $L/D = 0.4$ to an asymptotic value of $\langle z \rangle \sim 10$ for rods of $L/D > 30$, as shown in Fig. 6.6, demonstrating that the predictions of previous numerical simulations are incorrect [89]. The data

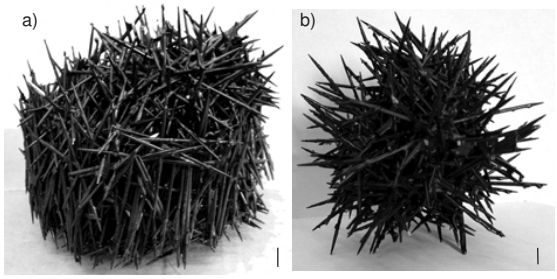

Figure 6.4: The compacted pile of $L/D = 32$ rods is shown after painting, drying and removal from the container. Panel a) shows the entire pile and panel b) shows the pile after the boundary rods have been removed. The scale bars indicate 1 cm.

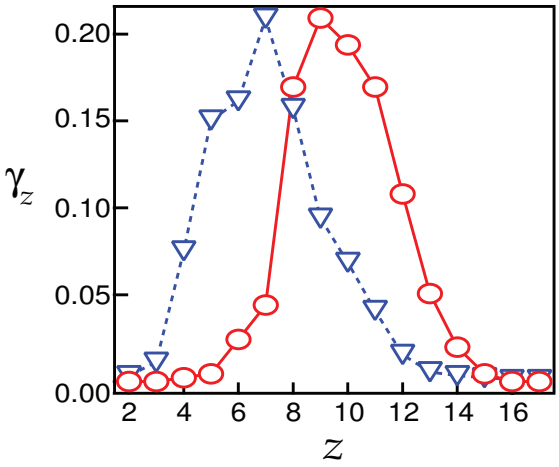

Figure 6.5: The co-ordination number distribution function of 454 bulk rods is shown as open circles alongside the distribution for the 904 boundary rods which is shown as open triangles, for a compacted pile of $L/D = 32$ rods.

on spheres [86] and on ellipsoids [78] is also displayed. As shown in Table 6.1 we find that $\langle z \rangle$ increases when a random packing of rods is compacted. For compacted piles of long aspect ratio rods the number of touching neighbors, $\langle z \rangle$, approaches the value for isostatic frictionless non-spherical particles, $\langle z_n^{\mathrm{iso}} \rangle = 10$. Fig. 6.6 shows that $\langle z \rangle$ for rods increases gradually as a function of aspect ratio without any singular behavior at $L/D = 1$, whereas Donev *et al.* [78] find that $\langle z \rangle$ is singular about $L/D = 1$. Furthermore, $\langle z \rangle$ increases approximately ten times more rapidly for ellipsoids than for cylinders. Why do packings of cylinders and ellipsoids behave so differently? Ellipsoids with aspect ratios different than one are not spherically symmetric while ellipsoids of aspect ratio equal to one are spherically symmetric. Therefore the steep variation in $\langle z \rangle$ as a function of aspect ratio seen by Donev *et al.* [78] arises due to the transition from spherical to ellipsoidal symmetry. However, cylindrical particles of different aspect ratios have the same symmetry and therefore no singular behavior of $\langle z \rangle$ as a function of aspect ratio is expected for rods. It is possible that friction between our experimental cylinders also contributes to the striking difference in the dependence of $\langle z \rangle$ as a function of aspect ratio for rods and simulated frictionless ellipsoids [78]. However, Philipse [15] showed that the bulk behavior of compacted piles of granular rods does not depend on the frictional properties of the rods. This leads us to conclude that the geometrical difference between cylinders and ellipsoids is responsible for the differences in co-ordination number, not friction. Simulations which could systematically vary the friction would be able to discriminate between these two hypotheses.

If the geometry of granular cylinders dominates their behavior in compacted piles, then the RCM's prediction should hold in the long rod limit, namely that $\frac{\langle z \rangle}{\phi(V_{\mathrm{ex}}/V_{\mathrm{p}})} = 1$. The data from Table 6.1 allow us to test this quantitative prediction. In Fig. 6.10 the quantity $\frac{\langle z \rangle}{\phi(V_{\mathrm{ex}}/V_{\mathrm{p}})}$ is plotted as a function of L/D for bulk particles in compacted piles and shows that the RCM limit is approached for high aspect ratio

	$\langle z \rangle \pm 0.3$		$\phi \pm 0.04$	
L/D	uncomp	comp	uncomp	comp
0.4	-	5.7	-	0.56
1	-	6.2	-	0.70
3	-	5.7	-	0.58
15	6.5	7.0	0.26	0.34
32	7.2	9.8	0.13	0.18
50	8.3	9.8	0.08	0.10

Table 6.1: The average number of touching neighbors $\langle z \rangle$ and the volume fraction of the pile occupied by rods ϕ are listed as a function of rod aspect ratio L/D. Only the bulk rods are included. The column labelled as "uncomp" corresponds to the uncompacted random rod packings whereas the column labelled as "comp" corresponds to the compacted packings.

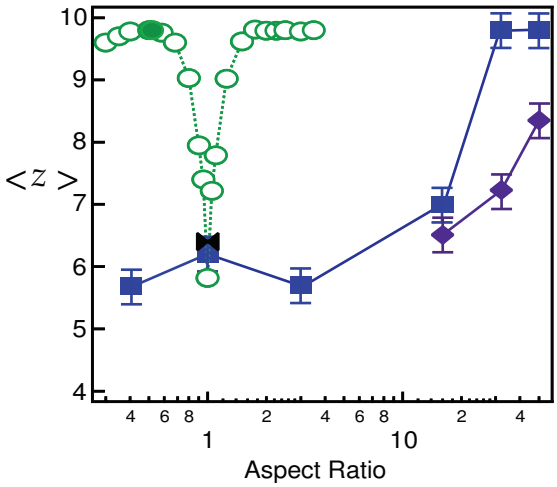

Figure 6.6: The average number of touching neighbors $\langle z \rangle$ is shown as a function of the aspect ratio (L/D) on a logarithmic scale. The squares (■) represent our compacted rod piles and the diamonds (♦) our uncompacted rod piles. The bowtie (⋈) represents spheres and is taken from Bernal & Mason [86]. The circles represent data on ellipsoids taken from Donev *et al.* [78]; the solid circle (•) is for M&Ms and the open circles (○) are from simulations.

cylindrical particles. This is further evidence that particle geometry and not friction determines piles of granular rods. The RCM assumes that contacts between rods are uncorrelated, that the excluded volume is given by the value for a pair of particles and is independent of volume fraction, and that rods are randomly oriented. Fig. 6.10 shows deviation from the RCM scaling for short rods and disks implying that some of these assumptions break down. Qualitatively, at least, the assumption of an isotropic angular distribution of rods is borne out experimentally, but we were not able to ascertain whether or not the two other assumptions were valid.

Philipse [15] noted that random packings of sufficiently high aspect ratio rods form solid-like plugs. One of the original motivations for performing the experiments described in this chapter was to test whether or not the value of the co-ordination number is related to plug formation. We observed plug formation only for compacted piles composed of rods with $L/D > 44$ as shown in Fig. 6.7. The plugs become more rigid as the aspect ratio of the rods increases. For all the plugs it was observed that rods are free to translate along their long axis. Rotation of a plug results in many rods falling out along the direction of their long axis. We measured $\langle z \rangle$ for the plug forming pile of bamboo skewers at $L/D = 50$ shown in Fig. 6.8. The data in Table 6.1 show that $\langle z \rangle$ is larger for the plug forming pile at $L/D = 50$ than for the uncompacted pile which did not form a solid-like plug. However, this value of $\langle z \rangle = 9.8$ was observed for the compacted pile at $L/D = 32$ which did not form a plug and for M & M's with aspect ratio of two [78] which shows that a certain value of $\langle z \rangle$ is necessary but not sufficient for plug formation. The co-ordination number distribution functions for the compacted piles at $L/D = 32$ and 50 are compared in Fig. 6.9. These distribution functions are almost identical with the only difference between the plug forming pile at $L/D = 50$ and the non-plug forming pile at $L/D = 32$ being the appearance of a second peak in the distribution function for $L/D = 50$. The distribution functions shown in Fig. 6.9 are similar to the

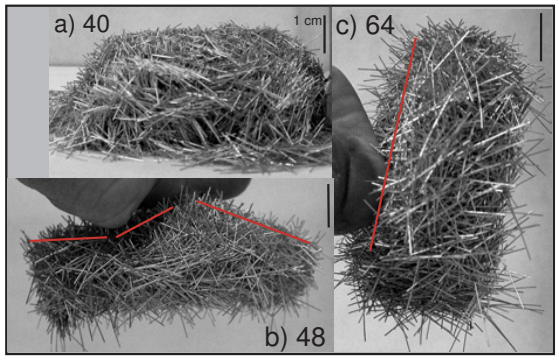

Figure 6.7: Piles of granular rods of sufficiently large aspect ratio ($L/D > 44$) form solid-like plugs as mentioned by Philipse [15]. Panel a) shows a compacted pile of $L/D = 40$ rods which does not form a plug. Panel b) shows a compacted pile of $L/D = 48$ rods which does form a plug which displays extensional rigidity. Note that in panel b) the surface normal of the plug deforms with mild applied stress as indicated by the lines. Panel c) shows a compacted pile of $L/D = 64$ rods which forms a more rigid plug than the pile of $L/D = 48$ rods. The pile of $L/D = 64$ rods can be rotated as a solid body as shown and the surface normal does not deform under mild applied stress.

distribution function measured for M&M's [78] so the appearance of this second peak in $\gamma(z)$ for $L/D = 50$ is likely not significant. These observations prove that a high value of $\langle z \rangle$ alone is not sufficient for plug formation. The mechanism leading to plug formation of granular rods remains unknown, but probably friction and flexibility of the cylinders are important physical variables.

6.4 Conclusion

In conclusion, we measured the average co-ordination number $\langle z \rangle$ for random piles of granular cylinders. $\langle z \rangle$ increases as the aspect ratio grows from $L/D = 1$. The increase in $\langle z \rangle$ was markedly slower for frictional cylinders than for simulations of frictionless ellipsoidal particles [78]. Furthermore frictional cylinders show no singular behavior at $L/D = 1$, in contrast to the frictionless simulated ellipsoids [78]. The co-ordination number of frictional cylinders reaches $\langle z \rangle \sim 10$ in the large aspect ratio

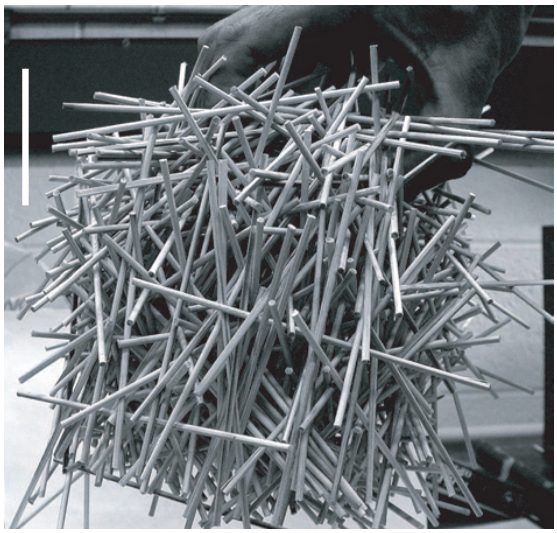

Figure 6.8: The compacted pile of $L/D = 50$ rods forms a solid plug. The pile is shown before $\langle z \rangle$ was measured. The white scale bar indicates 5cm.

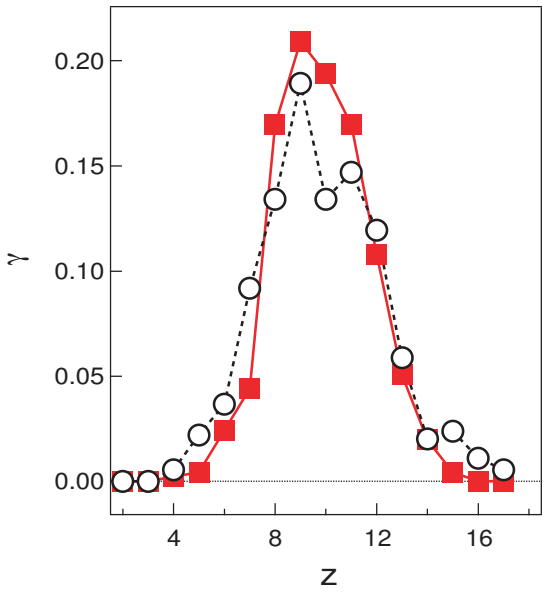

Figure 6.9: The co-ordination number distribution function $\gamma(z)$ is shown for the compacted pile of $L/D = 32$ rods (filled squares) and for the compacted, plug forming pile of $L/D = 50$ rods (open circles). As shown in Table 6.1, the measured value of $\langle z \rangle$ is the same for these two piles. Comparing their co-ordination number distribution function shows only one statistically significant difference: the appearance of a second peak in $\gamma(z)$ for $L/D = 50$. The small increase at $\gamma(z = 15)$ for $L/D = 50$ is not statistically significant.

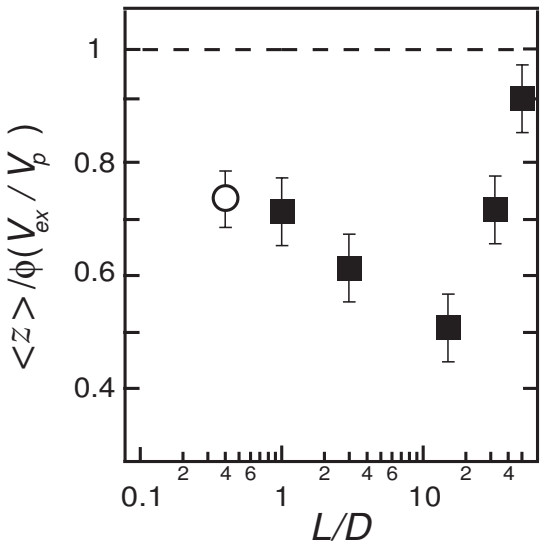

Figure 6.10: The measured data are shown along with the RCM's prediction for Eq. (1.15). The data for rods (■) and discs (○) from co-ordination number experiments is shown as a function of L/D for compacted piles. In the long rod limit the experimental data tend toward the RCM prediction; $\frac{\langle z \rangle}{\phi(V_{\rm ex}/V_{\rm p})} = 1$.

limit, $L/D \geq 30$, in compacted, random piles. Independent measurements of the volume fraction (ϕ) for these random rod packings coupled with measurements of the co-ordination number show that the random contact model is within a factor of two of experiment, and that theory and experiment approach each other in the long rod limit.